Dephasing-assisted parameter estimation in the presence of dynamical decoupling

Qing-Shou Tan,[1] Yixiao Huang,[1] Le-Man Kuang,[2] and Xiaoguang Wang[1,*]

[1]*Zhejiang Institute of Modern Physics, Department of Physics, Zhejiang University, Hangzhou 310027, China*

[2]*Key Laboratory of Low-Dimensional Quantum Structures and Quantum Control of Ministry of Education and Department of Physics, Hunan Normal University, Changsha 410081, China*

(Received 28 May 2013; published 4 June 2014)

We study the dephasing-assisted parameter estimation precision (PEP) enhancement in an atom interferometer with dynamical decoupling (DD) pulses. Through calculating the spin squeezing (SS) and the quantum Fisher information, we find that dephasing noise can improve PEP by inducing SS, and the DD pulses can maximize the improvement. It is indicated that when using the DD pulse the dephasing-induced SS can reach the limit of "one-axis twisting" model $\xi^2 \simeq N^{-2/3}$ with ξ^2 being the SS parameter and N the number of atoms. In particular, we find that the DD pulses can amplify the dephasing-induced quantum Fisher information by a factor of $\simeq N/2$ compared with the noise-free case, which means that under the control of DD pulses, the dephasing noise can enhance the precision of parameter estimation to the scale of $\sqrt{2}/N$, the same scale of the Heisenberg limit $(1/N)$.

DOI: 10.1103/PhysRevA.89.063604 PACS number(s): 03.75.Dg, 03.65.Ta, 06.20.Dk, 03.65.Yz

I. INTRODUCTION

Atom interferometry has attracted much attention because of its potential applications in quantum metrology [1–9]. Atomic Bose-Einstein condensates (BECs) are viewed as the ideal sources for an atom interferometer, due to their unique coherence properties and the possibility to yield controlled nonlinearity [10,11]. The nonlinearity of BECs caused by interatomic interactions can create squeezed states [12–17], which can improve the precision of parameter estimation (PPE).

The ability of BECs to create highly squeezed states and serve as nonlinear interferometers, whose precision exceeds the standard quantum limit (SQL) achieved with coherent spin states (CSS), has been demonstrated in two recent experiments [4,5]. However, the atom-atom nonlinear interaction strength caused by s-wave scattering is usually very small when the modes of the BEC have a spatial overlap [4,5,8]. Such nonlinearity enhancement currently resorts to the use of Feshbach resonances [4] or spatially separating the components of BEC [5], but the price of these methods is significantly increased atom losses, limiting the achievable squeezing. In Ref. [6], the authors proposed an approach to drastically enhance the nonlinear dynamics of the BEC based on collisions of the BEC with a thermal reservoir. This enhanced nonlinear interaction stems from the decoherence noise, which implies that the reservoir noise can also be regarded as a resource to improve the parameter estimation sensitivity. However, it is well known that the decoherence typically plays a coherence-destructive role which is one of the main obstacles to producing certain spin-squeezed states. Much research showed that the decoherence may prevent the production of certain spin-squeezed states and limit the precision of quantum metrology [18–24]. Thus, it is important to suppress the coherence-destructive role but at the same time maintain the decoherence-induced nonlinearity interaction if one wants to obtain a strong squeezing and improve PPE.

The dynamical decoupling (DD) technique [25–34], which has been widely employed in the area of quantum information, provides an active way to fight against decoherence. Recently, this technique has also been introduced into the field of magnetometers to improve the sensitivity of oscillating magnetic fields based on nitrogen-vacancy centers [35–38]. Combining the DD technique with quantum metrology can preserve PPE in noisy systems by suppressing the decoherence effect [34]. Thus a natural question arises: Is it possible to realize decoherence-enhanced PPE under the DD pulses?

In this paper, we give a positive answer to the above question by investigating the influence of the DD pulses on the spin squeezing (SS) and quantum Fisher information (QFI) [16,39–45], which are two important quantities relevant in parameter estimation [16,44]. We compare the effects of two different DD-pulse sequences: periodic DD (PDD) sequence [25,26] and Uhrig DD (UDD) sequence [28,29]. Our findings show that both these sequences can effectively suppress the coherence-destructive role while maintaining the decoherence-induced nonlinearity interaction. It is also found that in contrast to the PDD sequence the UDD sequence can work more efficiently, which can enhance the decoherence-induced SS to the limit of $\xi^2 \simeq N^{-2/3}$ [14,15] more easily, where ξ^2 is the SS parameter and N is the number of atoms. In particular, we find that it is possible for the UDD sequence to amplify the QFI by a factor of $\simeq N/2$ compared with the initial CSS in the case of pure dephasing. It means that the dephasing-assisted sensitivity of the estimated parameter can be enhanced from the SQL $1/\sqrt{N}$ to $\sqrt{2}/N$, which approaches nearly Heisenberg-limited precision $(1/N)$ [46,47].

This paper is organized as follows. In Sec. II, we introduce our physical model and Hamiltonian under control pulses. We then investigate the dynamical evolution of the BEC system in the dephasing environment with two different DD-pulse sequences. In Sec. III, we study the effects of DD pulses on the SS enhancement. In Sec. IV we discuss the dephasing-assisted QFI amplification by using the DD pulses. It is found that the UDD pulses can greatly amplify the QFI and enhance the PPE to the scale of Heisenberg limit. Finally, we conclude this work in Sec. V.

*xgwang@zimp.zju.edu.cn

II. DEPHASING IN TWO-COMPONENT BOSE-EINSTEIN CONDENSATE SYSTEM WITH DD-PULSE SEQUENCES

In this section, we present the model used to study a two-component BEC interacting with an external field in a dephasing reservoir which models the effect of background thermal atoms on the two-component BEC. We investigate the dynamical evolution of the two-component BEC in the dephasing reservoir under two different DD-pulse sequences: PDD sequence and UDD sequence. The two-component BEC system under our consideration is available from several recent experimental systems properly involving two different magnetic sublevels of an atom [4,5,48,49].

A. Model and Hamiltonian

We consider a two-component BEC in two different hyperfine states $|A\rangle$ and $|B\rangle$ coupled by a Raman laser or microwave field. Under the resonant condition, the Hamiltonian of this system is given by [50]

$$H_S = H_A + H_B + H_E, \tag{1}$$

$$H_i = \int d\mathbf{x}\, \hat{\psi}_i^\dagger(\mathbf{x}) \left[-\frac{\nabla^2}{2m} + V_i(\mathbf{x}) + \sum_j \frac{U_{ij}}{2} \hat{\psi}_j^\dagger(\mathbf{x}) \hat{\psi}_j(\mathbf{x}) \right] \hat{\psi}_i(\mathbf{x}), (i,j) = (A,B), \tag{2}$$

$$H_E = \frac{1}{2} \int d\mathbf{x} [\Lambda \hat{\psi}_A^\dagger(\mathbf{x}) \hat{\psi}_B(\mathbf{x}) + \Lambda^* \hat{\psi}_B^\dagger(\mathbf{x}) \hat{\psi}_A(\mathbf{x})], \tag{3}$$

where $\hat{\psi}_i(\mathbf{x})$ and $\hat{\psi}_i^\dagger(\mathbf{x})$ are the atomic field operators in the hyperfine state $|i\rangle$ $(i = A,B)$, which annihilate and create atoms at position $\mathbf{x}$, respectively. The trapping potential for atoms in state $|i\rangle$ is denoted by $V_i(\mathbf{x})$ and their mass is m. The interaction strengths are given by U_{AA}, U_{BB}, and U_{AB} for collisions between particles in state $|A\rangle$, state $|B\rangle$, and interspecies collisions, respectively. Λ is the effective Rabi frequency. It should be pointed out that here we neglect the effects of three-body recombination [51–56], which is the intrinsic particle loss mechanism of BEC, and strong dependents on the s-wave scattering length, atom density, and external magnetic field. In fact, when the system with low densities is far away from a Feshbach resonance regime, the effects of the three-body recombination can be neglected in comparison to U_{ij} [55]. Furthermore, these effects can be inhibited by using an external magnetic field or resonant laser pulses [55].

For a weakly interacting BEC at low temperature the thermally excited atoms and the quantum depletion are negligible, and the motional state is frozen to be approximately the ground state. One may neglect all modes except for the condensate mode and take the so-called single-mode approximation of the atomic field operators as $\hat{\psi}_A(\mathbf{x}) \approx a\varphi_A(\mathbf{x})$ and $\hat{\psi}_B(\mathbf{x}) \approx b\varphi_B(\mathbf{x})$, where $\varphi_i(\mathbf{x})$ $(i = A,B)$ is a normalized wave function for the atoms in the BEC in the internal state $|i\rangle$, and a and b are usual bosonic annihilation operators which obey bosonic commutation relations $[a,a^\dagger] = 1$, $[b,b^\dagger] = 1$, $[a,b^\dagger] = 0$, and $[a,b] = 0$. Under the single-mode approximation Hamiltonian (1) can be written as [57,58]

$$H_S = \omega_A a^\dagger a + \omega_B b^\dagger b + \frac{\Omega}{2}(a^\dagger b + a b^\dagger) + u_{AB} a^\dagger a b^\dagger b + \frac{u_{AA}}{2} a^{\dagger 2} a^2 + \frac{u_{BB}}{2} b^{\dagger 2} b^2, \tag{4}$$

where the relevant parameters are given by

$$\omega_i = \int d\mathbf{x}\, \varphi_i^*(\mathbf{x}) \left[-\frac{\nabla^2}{2m} + V_i(\mathbf{x}) \right] \varphi_i(\mathbf{x}) \quad (i = A,B),$$
$$u_{ij} = U_{ij} \int d\mathbf{x} |\varphi_i(\mathbf{x})|^2 |\varphi_j(\mathbf{x})|^2 \quad (i,j = A,B), \tag{5}$$
$$\Omega = \Lambda \int d\mathbf{x}\, \varphi_A^*(\mathbf{x}) \varphi_B(\mathbf{x}).$$

We define the angular momentum operators in terms of the BEC operators in the usual way: $J_x = (a^\dagger b + a b^\dagger)/2$, $J_y = (a b^\dagger - a^\dagger b)/(2i)$, and $J_z = (b^\dagger b - a^\dagger a)/2$; the Hamiltonian of the two-component BEC given by Eq. (4) reduces to the "one-axis twisting" (OAT) Hamiltonian [14]

$$H_S = \Omega J_x + \lambda J_z + \chi J_z^2, \tag{6}$$

where the relevant parameters are given by

$$\lambda = \omega_B - \omega_A + (u_{BB} - u_{AA})(\hat{N} - 1)/2,$$
$$\chi = (u_{BB} + u_{AA} - 2u_{AB})/2. \tag{7}$$

Here we have neglected the constant energy shift, which depends on the number operator $\hat{N} = a^\dagger a + b^\dagger b$. In Eq. (7), χ is the effective nonlinearity arising from intra- and interspecies interaction, determined by the s-wave scattering lengths u_{ij} $(i,j) = (A,B)$.

It is interesting to note that the OAT Hamiltonian (6) has been realized by two groups [4,5] in two nice experiments on quantum metrology based on two-component BECs. In these experiments, three scattering lengths u_{ij} $(i,j) = (A,B)$ are very close. The ratio of three scattering lengths is $u_{AA} : u_{BB} : u_{AB} = 100 : 97.7 : 95$ in experiments [4], and $u_{AA} : u_{BB} : u_{AB} = 100.4 : 95.0 : 97.7$ in experiments [5]. It results in only a very small effective nonlinear interaction denoted by χJ_z^2 which can be neglected when the system is in the Rabi regime with $\chi N/\Omega \ll 1$. It should be pointed out that $\chi \simeq 0$ indicates that intraspecies nonlinear interactions cancel out interspecies nonlinear interactions in the two-component BEC. This does not imply the neglect of interatomic interactions in the two-component BEC in our model. This point can be easily seen from Eq. (7) which indicates $\chi \simeq 0$ when $u_{BB} + u_{AA} \simeq 2u_{AB}$.

We next investigate the effects of decoherence on the BEC system. For the BEC system under our consideration the dominant source of decoherence is due to the background atoms [50,57–60]. There are two relevant types of two-body interaction between the condensed and background atoms: elastic interactions which preserve the number of condensate atoms and inelastic interactions which do not. The former produces phase damping, i.e., dephasing, and dominates when there is only a small number of thermal atoms with sufficient energy to knock atoms out of the condensate, that is, for temperatures low enough that the fugacity is small compared to 1 [59].

Here we give a brief analysis about the temperature limitations of the negligible particle-number fluctuations $\delta^2 N_0$ [61–64] in our model, with N_0 being the average particle number in condensate. When the temperature T is below the critical temperature T_c, for ideal Bose gas confined in a harmonic trap, there is a very good approximation for the particle-number fluctuations in the condensate [61]: $\langle \delta N_0^2 \rangle^{\mathrm{IBG}} = \frac{\pi^2}{6\zeta(3)} N (T/T_c)^3$ [here N is the total atom number considered and $\zeta(3) \approx 1.202$ is the Riemann zeta function [62]]. This analytic expression can give us the request of the temperature to neglect the effects of particle-number fluctuations. In our model, it is clear that we should request $\delta N_0/N_0 \ll 1$. From $N_0/N = 1-(T/T_c)^3$, we have the following requirement for the temperature of the system: $(T/T_c)^{3/2}/[1-(T/T_c)^3] \ll \sqrt{6\zeta(3)N}/\pi$. For an ultracold atomic system with N the order of $\sim 10^3$, when $T/T_c < 0.5$ the above request can be always satisfied. Note that for microcanonical the particle-number fluctuations can be further reduced, and hence our scheme can work better [64].

Hence, in the above temperature limitations, we can only consider the effects of dephasing. We model the reservoir of the condensed atoms by the use of a system of harmonic oscillators with the creation and annihilation operators $c_k^\dagger$ and c_k [6]. The Hamiltonian of the reservoir is given by

$$H_R = \sum_k \omega_k c_k^\dagger c_k, \tag{8}$$

where ω_k is the frequency of the oscillator for the kth reservoir mode. The dephasing-interaction Hamiltonian between the BEC and the reservoir can be described by [6,32,65–67]

$$H_I = J_z \sum_k g_k (c_k^\dagger + c_k), \tag{9}$$

which describes the dephasing interaction induced by elastic collisions between the BEC atoms and background atoms or phonons.

Below, we show that the coherence-destructive effect produced by the dephasing interaction can be suppressed while preserving the decoherence-induced nonlinearity interaction by the use of DD-pulse sequences. A DD-pulse sequence consists of n DD π pulses, which split the total time interval t into $n+1$ small intervals t_j with $t_0 = 0$ and $t_{n+1} = t$. Each ideal DD π pulse corresponds to $\Omega(\tau) = \Omega_0 \delta(\tau - t_j)$ and $\int_{t_j-\sigma}^{t_j+\sigma} \Omega(s) ds = \pi$ with $\tau \in [0,t]$ and $\sigma \to 0$, which transforms $e^{i\pi J_x} J_z e^{-i\pi J_x} = -J_z$ at time t_j.

In the interaction picture with respect to H_R, the total Hamiltonian with DD pulse is

$$H_I(\tau) = \lambda \varepsilon(\tau) J_z + \chi J_z^2 + \varepsilon(\tau) J_z \sum_k g_k (b_k^\dagger e^{i\omega_k \tau} + b_k e^{-i\omega_k \tau}), \tag{10}$$

where the switch function $\varepsilon(\tau)$ changes the sign of J_z (i.e., $J_z \to -J_z$) at time t_j, which is denoted by

$$\varepsilon(\tau) = \sum_{j=0}^{n} (-1)^j \theta(\tau - t_j)\theta(t_{j+1} - \tau), \tag{11}$$

with $\theta(x)$ the Heaviside step function.

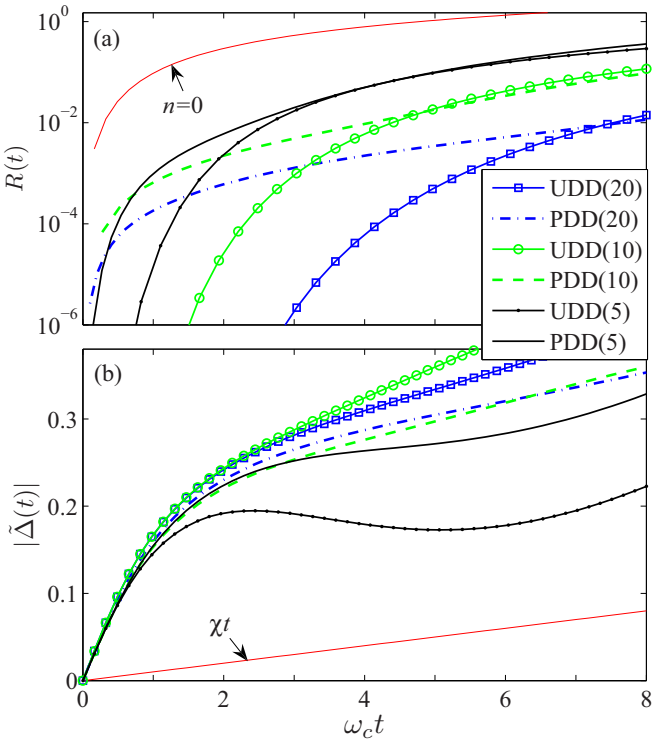

FIG. 1. (Color online) Comparison of dynamical behaviors of functions $R(t)$ and $|\tilde{\Delta}(t)| \equiv |\Delta(t) + \chi t|$ under two different DD-pulse sequences. Relevant parameters are chosen as coupling strength $\alpha = 0.02$, $\chi = 0.01$, and temperature $T = 0.5\omega_c < 0.5T_c$.

Thus, the time evolution operator can be obtained by using Magnus expansion [6,68]

$$\begin{aligned} U(t) &= T_+ \exp\left[-i \int_0^t H_I(t')dt'\right] \\ &= \exp\left\{-i\left[\phi(t) J_z + \tilde{\Delta}(t) J_z^2\right]\right\} V(t) \end{aligned} \tag{12}$$

with T_+ the time ordering, where $\phi(t) = \int_0^t \lambda \varepsilon(\tau) d\tau$, and

$$\begin{aligned} &\tilde{\Delta}(t) \equiv \Delta(t) + \chi t, \\ &\Delta(t) = \sum_k g_k^2 \int_0^t d\tau \int_0^\tau d\tau' \varepsilon(\tau)\varepsilon(\tau') \sin\omega_k(\tau' - \tau), \\ &V(t) = \exp\left[J_z \sum_k (\alpha_k b_k^\dagger - \alpha_k^* b_k)\right], \end{aligned} \tag{13}$$

with the amplitudes $\alpha_k = -i g_k \int_0^t e^{i\omega_k \tau} \varepsilon(\tau)\, ds$. Here $\Delta(t)$ is the noise-induced nonlinearity interaction, and for small χt we have $\Delta(t) \approx \tilde{\Delta}(t)$, which means that the nonlinear effect can be drastically enhanced by the dephasing noise [see Fig. 1(b)].

B. System dynamical evolution under DD-pulse sequences

Now, we investigate the dynamical evolution of the BEC system, which suffers from dephasing noise with the DD-pulse sequences. Assuming that the initial state ($t = 0$) of the total system is given by

$$\rho_T(0) = |\Psi(0)\rangle_S \langle \Psi(0)| \otimes \rho_B, \tag{14}$$

where $|\Psi(0)\rangle_S = \sum_m c_m(0)\,|j,m\rangle$ is the CSS, with the probability amplitudes $c_m = 2^{-j}(C_{2j}^{j+m})^{1/2}$ and total spin $j = N/2$ for a system consisting of N condensate atoms. Such a state is the optimal initial state to obtain the strongest squeezing [14,15]. In Eq. (14), ρ_B is the thermal equilibrium state of the reservoir, defined by

$$\rho_B = \Pi_k[1-\exp(-\beta\omega_k)]\exp(-\beta\omega_k b_k^\dagger b_k), \tag{15}$$

with β the inverse temperature ($\beta = 1/k_BT$; hereafter we set the Boltzmanm constant $k_B = 1$).

Based on Eq. (12), the time-evolution reduced matrix elements of the BEC system can be determined from the relation

$$\begin{aligned}\rho^S_{jm,jl}(t) &= \mathrm{Tr}_B[\langle j,m|\,U(t)\rho(0)U^{-1}(t)\,|j,l\rangle] \\ &= e^{-i\phi(t)(m-l)}e^{-i(m^2-l^2)\tilde{\Delta}(t)}e^{-(m-l)^2R(t)}\rho_{jm,jl}(0).\end{aligned} \tag{16}$$

In Eq. (16), the decoherence function with n DD pulse (see Appendix A for details)

$$R_n(t) = \int_0^\infty d\omega\, F_n(\omega,t)G(\omega) \tag{17}$$

is the overlap integral of the filter function

$$F_n(\omega,t) = \frac{1}{2\omega^2}\left|1+(-1)^{n+1}e^{i\omega t} + 2\sum_{j=1}^{n}(-1)^j e^{i\omega t_j}\right|^2, \tag{18}$$

and the temperature-dependent interacting spectrum

$$G(\omega) = J(\omega)[2n(\omega)+1] = J(\omega)\coth(\beta\omega/2), \tag{19}$$

where $J(\omega)$ is the spectral density and $n(\omega) = [\exp(\beta\omega)-1]^{-1}$ is the bosonic distribution function of the heat reservoir.

Substituting the spectral density $J(\omega) = \sum_k g_k^2(\omega-\omega_k)$ into Eq. (13), then the noise-induced nonlinear term with n DD pulse can be rewritten as (see Appendix B)

$$\Delta_n(t) = \int_0^\infty d\omega\, J(\omega) f_n(\omega,t), \tag{20}$$

with

$$\begin{aligned} f_n(\omega,t) &= \vartheta_n(\omega,t) + \mu_n(\omega,t) - t/\omega, \\ \vartheta_n(\omega,t) &= \frac{1}{\omega^2}\left[2\sum_{m=1}^{n}(-1)^m\sin(\omega t_m) + (-1)^{n+2}\sin(\omega t)\right], \\ \mu_n(\omega,t) &= \frac{2}{\omega^2}\left\{\sum_{m=1}^{n}\sum_{j=1}^{m}(-1)^{m+j}(\sin[\omega(t_{m+1}-t_j)]\right. \\ &\quad \left. -\sin[\omega(t_m-t_j)])\right\}, \end{aligned} \tag{21}$$

which is temperature independent. Note that the result attained in the above equation is more complex than that in Ref. [28] for the single-qubit DD case.

When restricting our discussion in the one-dimensional trap, then the spectral density of the heat reservoir can be expressed in the Ohmic form

$$J(\omega) = \alpha\omega e^{-\omega/\omega_c}, \tag{22}$$

where α is the coupling strength between the system and the reservoir and ω_c is the cutoff frequency. According to Eqs. (17) and (20), we find in the absence of control ($n = 0$) [67,69,70],

$$\begin{aligned} R_0(t) &= \alpha\int_0^\infty d\omega\,\omega e^{-\omega/\omega_c}\coth(\beta\omega/2)\frac{1-\cos(\omega t)}{\omega^2}, \\ \Delta_0(t) &= \alpha[\arctan(\omega_c t) - \omega_c t], \end{aligned} \tag{23}$$

where the decoherence function $R(t)$ can be further reduced as

$$R_0(t) = \alpha\left\{\frac{1}{2}\ln\left(1+\omega_c^2t^2\right) + \ln\left[\frac{\beta}{\pi t}\sinh(\pi t/\beta)\right]\right\} \tag{24}$$

in the low temperature case ($\beta\omega_c \gg 1$).

For the PDD sequences, in which the π pulse is applied at equidistant intervals

$$t_j^{\mathrm{PDD}} = jt/(n+1), \tag{25}$$

the modulation spectrums $F_n(\omega,t)$ and $f_n(\omega,t)$ in Eqs. (17) and (20) can be, respectively, given by [28]

$$\begin{aligned} F_n^{\mathrm{PDD}}(\omega,t) &= \tan^2[\omega t/(2n+2)][1+(-1)^n\cos(\omega t)]/\omega^2, \\ f_n^{\mathrm{PDD}}(\omega,t) &= \frac{2(-1)^{n+1}\sin(\omega t)+\omega t}{\omega^2} \\ &\quad + 2\tan\left(\frac{\omega t}{2n+2}\right)\frac{(-1)^n\cos(\omega t)-n}{\omega^2} \\ &\quad + \tan^2\left(\frac{\omega t}{2n+2}\right)\frac{(-1)^n\sin(\omega t)}{\omega^2}. \end{aligned} \tag{26}$$

Whereas for the UDD sequences [28]

$$t_j^{\mathrm{UDD}} = t\,\sin^2\left[j\pi/(2n+2)\right], \tag{27}$$

the filter function is

$$F_n^{\mathrm{UDD}}(\omega,t) \approx 8(n+1)^2J_{n+1}^2(\omega t/2)/\omega^2, \tag{28}$$

where $J_n(x)$ is the Bessel function and has $(n+1)J_{n+1}^2(x) \propto [x/(n+1)]^{2n+2}$ manifesting the effects of the vanishing leading derivatives [28]. The function $f_n^{\mathrm{UDD}}(\omega,t)$ can also be attained by inserting t_j^{UDD} into Eq. (21).

It is worth noting that although both the functions of $R(t)$ and $\Delta(t)$ stem from environment noise, they play different roles. In other words, $\Delta(t)$ can induce the quantum correlation in the system, while $R(t)$ destroys it. These results imply that if one wants to make full use of the advantage of environment noise to enhance the desired quantum correlation, the coherence-destructive process must be suppressed. Fortunately, from Fig. 1, it is found that the DD pulse can effectively average the decoherence function $R(t)$ nearly to zero, but does not completely remove the noise-induced nonlinear term $\Delta(t)$ [i.e., $\tilde{\Delta}(t) > \chi t$].

Moreover, from Fig. 1 we can find that the UDD sequences are more effective when used to suppress the decoherence function $R(t)$. The reason can be explained as follows. From Eq. (26), it is clear that PDD can only eliminate $F_n^{\mathrm{PDD}}(\omega,t)$ up to $O(t^2)$ for a short duration, which means $R^{\mathrm{PDD}}(t) \sim O(t^2)$, while from Eq. (28) we find that UDD can eliminate $F_n^{\mathrm{UDD}}(\omega,t)$ up to $O(t^{2n+2})$ [i.e., $R^{\mathrm{UDD}}(t)(\omega,t) \sim O(t^{2n+2})$] for a short duration, and only needs n pulses [28]. Thus, the UDD sequences can greatly eliminate the coherence-destructive

process when the same number of pulses are applied. In fact, the UDD is the most efficient sequence to eliminate pure dephasing, for that is the best way to make the first n derivatives of $\varepsilon(\omega,t)$ vanish, while requiring only linear number of pulses [28,29].

Next, we will investigate how to obtain the best squeezing and QFI, which are two quantities relevant in interferometry, in the presence of dephasing by using DD-pulse sequences. Additionally, we also demonstrate the advantage of UDD sequences.

III. SPIN SQUEEZING IN THE PRESENCE OF DEPHASING UNDER DD-PULSE SEQUENCES

In this section, we shall evaluate the magnitude of the SS, and demonstrate how to improve it in the presence of dephasing by employing the DD schemes considered above. To quantify the degree of SS, we introduce the SS parameter given by Kitagawa and Ueda [14]:

$$\xi^2 = \frac{4(\Delta J_{\vec{n}_\perp})^2_{\min}}{N}, \tag{29}$$

where $(\Delta J_{\vec{n}_\perp})_{\min}$ represents the minimal variance of the spin component, which is over all directions denoted by $\vec{n}_\perp$, perpendicular to the mean spin direction.

With the use of Eq. (16), we can obtain the degree of SS for the initial state given in Eq. (14) in the case of pure dephasing noise

$$\xi^2 = 1 + \frac{N-1}{4}(A - \sqrt{A^2+B^2}), \tag{30}$$

in the optimally squeezed direction $\psi_{\rm opt} = [\pi + \tan^{-1}(B/A)]/2$, where

$$\begin{aligned} A &= 1 - \cos^{N-2}[2\tilde{\Delta}(t)]\exp[-4R(t)], \\ B &= -4\,\sin[\tilde{\Delta}(t)]\cos^{N-2}[\tilde{\Delta}(t)]\exp[-4R(t)]. \end{aligned} \tag{31}$$

Compared with Refs. [14,15], the controllable decoherence function $R(t)$ is introduced and the scaled time χt is replaced by $\tilde{\Delta}(t)$ in the above equations. From Eqs. (30) and (31), we can clearly find again that dephasing noise plays two roles: On one hand, it can generate the SS by enhancing the nonlinear interaction in $\tilde{\Delta}(t)$. In particular, when $\chi \simeq 0$ the SS is mainly generated by the noise-induced nonlinearity interaction $\Delta(t)$; on the other hand, it degrades the degree of SS via the decoherence function $R(t)$. However, from Eqs. (17), (26), and (28), it is found that if $t/(n+1) \to 0$, we have $R(t) \to 0$, then the coherence-destructive effect is suppressed. Therefore, in the short-time limit and the large particle number limit ($N \gg 1$), the best squeezing can be approximated as

$$\xi^2_{\min} \simeq \frac{3}{2N}\left(\frac{N}{3}\right)^{1/3} \simeq N^{-2/3}, \tag{32}$$

which is the well-known result appearing in Refs. [14,15] for the ideal noise-free case.

To clearly observe the effects of the DD pulses on SS, a comparison of the consequence for two different DD schemes on the dynamics of SS is given in Fig. 2. It indicates that both these DD sequences can effectively improve the magnitude of squeezing, and the UDD pulses work more efficiently than the

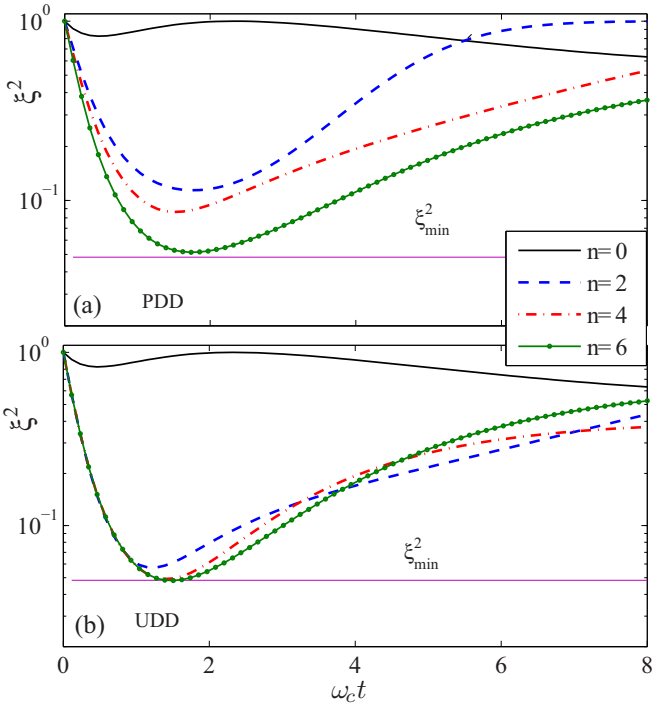

FIG. 2. (Color online) Spin squeezing ξ^2 with respect to scaled time $\omega_c t$ for the (a) PDD sequence and (b) UDD sequence with different numbers of control pulse n. Relevant parameters are chosen as $N = 100, \chi = 0.01, \alpha = 0.02$, and $T = 0.5\omega_c < 0.5T_c$. Here $\xi^2_{\min}$ is the approximations given in Eq. (32).

PDD pulses when they are used to enhance the SS; for the fixed pulse number the better squeezing can be obtained by applying a UDD pulse sequence. From Fig. 2, we can see that the strongest squeezing $\xi^2_{\min}$ for OAT given in Eq. (32) can be obtained if the number of DD pulses is large enough. This is an interesting phenomenon since this squeezing limit is usually thought to be achieved only in the ideal noise-free OAT case, but we find that it can be reached by the environment noise with DD-pulse sequences.

The SS characterizes the sensitivity of a state with respect to SU(2) rotations and has been studied in quantum metrology, which showed that the SS is a useful resource to improve PPE. Dephasing can induce the squeezing, which means that the dephasing noise also can be regarded as a resource to enhance the PPE, when self-interaction χ is very small.

IV. DEPHASING-ASSISTED QFI AMPLIFICATION IN THE PRESENCE OF DD PULSES

To better understand the behaviors of dephasing-assisted enhancement of parameter sensitivity, we evaluate the QFI F, which gives a theoretical-achievable limit on the precision of an unknown parameter θ via Cramér-Rao bound

$$\Delta\theta_{\min} = \frac{1}{\sqrt{\upsilon F}}, \tag{33}$$

with υ the number of measurements. Below, we set $\upsilon = 1$ for simplicity.

According to Refs. [8,42–45], the QFI F with respect to θ, acquired by an SU(2) rotation, can be explicitly derived as

$$F[\rho(\theta,t),J_{\vec{n}}] = \mathrm{Tr}\left[\rho(\theta,t)L_\theta^2\right] = \vec{n}\mathbf{C}\vec{n}^T, \tag{34}$$

where

$$\rho(\theta,t) = \exp(-i\theta J_{\vec{n}})\rho(t)\exp(i\theta J_{\vec{n}}) \tag{35}$$

and the matrix element for the symmetric matrix $\mathbf{C}$ is

$$\mathbf{C}_{kl} = \sum_{i\neq j}\frac{(p_i-p_j)^2}{p_i+p_j}[\langle i|J_k|j\rangle\langle j|J_l|i\rangle + \langle i|J_l|j\rangle\langle j|J_k|i\rangle], \tag{36}$$

where $p_i(|i\rangle)$ are the eigenvalues (eigenvectors) of $\rho(\theta,t)$.

In particular, if ρ is a pure state, the above matrix can be simplified as [42–45]

$$\mathbf{C}_{kl} = 2\langle J_kJ_l + J_lJ_k\rangle - 4\langle J_k\rangle\langle J_l\rangle. \tag{37}$$

From Eq. (34), one finds that to get the highest possible estimation precision $\Delta\theta$, a proper direction $\vec{n}$ should be chosen for a given state, which maximizes the value of the QFI. With the help of the symmetric matrix, the maximal QFI can be obtained as

$$F_{\max} = \lambda_{\max}, \tag{38}$$

where $\lambda_{\max}$ is the maximal eigenvalues of $\mathbf{C}$. And for the initial CCS we have $F_{\max}^{\mathrm{CSS}} = N$, then $\Delta\theta_{\min} = 1/\sqrt{N}$, which reaches SQL.

As discussed in the previous sections, the DD pulses can decouple the state of the system from environment by averaging the decoherence function $R(t)$ to zero. To further check its consequence, here we introduce the purity of a quantum state, which is defined by

$$P(\rho) \equiv \mathrm{Tr}(\rho^2). \tag{39}$$

The quantum state is pure if its purity takes the maximum value 1, while it is the maximally mixed state $\rho_m \equiv \mathbb{I}/D$ if its purity takes the minimum value $1/D$ with D being the dimension of the quantum system [71].

In Fig. 3, we give a comparison of the effects between UDD and PDD sequences for different values of α on protecting the purity of the quantum state. Figure 3 indicates the advantage of the UDD sequence in preserving the purity of a quantum state. In contrast to the PDD pulses, the UDD pulses can preserve the maximum value of purity for a longer time and the behavior for different couplings α does not change as obviously as in the case of PDD pulses. This feature of a UDD pulse means it has a long preservation time for maximal purity even with large coupling. Thus, we can obtain a pure state $[P(\rho) = 1]$ at certain times if the UDD pulses are applied. Figure 3 also indicates that a larger number of UDD pulses conduces longer preservation time of pure state, which implies that the coherent-destructive effect can be nearly completely suppressed.

We now investigate the influences of the number of UDD pulses as well as the temperature on the QFI amplification rate. Based on Eqs. (34)–(38), the maximal QFI amplification rate with respect to the initial state can be defined as

$$\eta = F_{\max}/F_{\max}^{\mathrm{CSS}} = \lambda_{\max}/N. \tag{40}$$

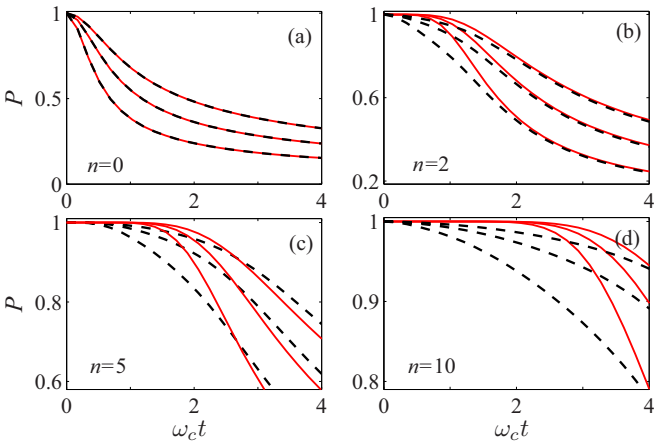

FIG. 3. (Color online) Purity defined in Eq. (39) vs time $\omega_c t$ for different numbers of DD pulse with $T = 0.5\omega_c < 0.5T_c$, $N = 100$, and $\chi = 0.05$. Solid (red) curves are for the UDD sequence and dashed (black) curves are for the PDD sequence. From the bottom to the top, the curves correspond to $\alpha = 0.05, 0.02$, and 0.01.

In Fig. 4, we plot the QFI amplification rate η as a function of scaled temperature T/ω_c for various numbers of UDD pulses. From Fig. 4(a) to Fig. 4(c), we can see that the QFI amplification rate significantly increases and its temperature dependence can be significantly suppressed with the number of UDD pulses. As can be seen, in the absence of DD pulses the amplification rate η decreases when increasing the scaled temperature T/ω_c [see Fig. 4(a)]. However, when increasing the number of DD pulses, η becomes insensitive to the change of T/ω_c. In particular, when increasing the number of DD pulses, the QFI amplification rate η increases gradually. As shown in Fig. 4(c), when $n = 15$ we can obtain the largest η and its value is almost independent of the temperature. These results can be explained as follows.

From Eq. (17) and Fig. 1(a) we can see that when the number of DD pulses is sufficiently large, the temperature-dependent term $R(t)$ is suppressed with $R(t) \to 0$. Hence the states given in Eq. (16) can approach a pure state with $P(\rho) \to 1$. In this case, based on Eqs. (37), (38), and (40) we can obtain

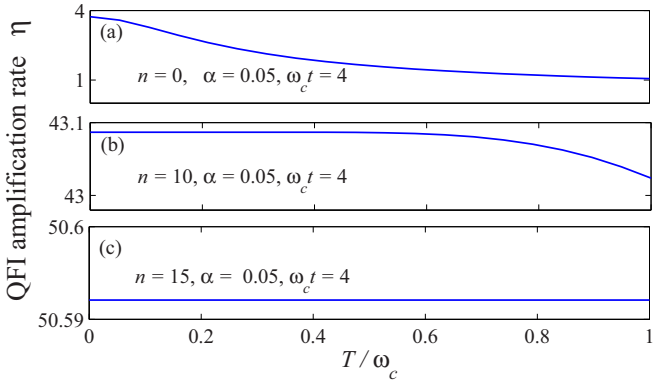

FIG. 4. (Color online) QFI amplification rate $\eta \equiv F_{\max}/N$ as a function of scaled temperature T/ω_c ($\omega_c > 2T_c$) for various numbers of UDD pulse: (a) $n = 0$, (b) $n = 10$, and (c) $n = 15$. Other relevant parameters are chosen as $N = 100, \omega_c t = 4$, $\chi = 0.01$, and $\alpha = 0.05$.

the explicit form of the maximal QFI amplification rate (see Appendix C):

$$\eta(N,t) = \max\left\{1 + \frac{N-1}{4}(A'_+ + \sqrt{A'^2_+ + B'^2}),\right.$$
$$\left. 1 + \frac{N-1}{2}A'_- - N\cos^{2N-2}[\tilde{\Delta}(t)]\right\}, \quad (41)$$

with

$$A'_\pm = 1 \pm \cos^{N-2}[2\tilde{\Delta}(t)],$$
$$B' = -4\sin[\tilde{\Delta}(t)]\cos^{N-2}[\tilde{\Delta}(t)]. \quad (42)$$

Clearly, Eq. (41) is independent of temperature T. Therefore, we can conclude that the QFI amplification rate can be significantly enhanced and the temperature influence can be sufficiently suppressed through increasing the number of UDD pulses.

Now we examine the validity of Eq. (41) in the presence of a UDD pulse. In Fig. 5(a), we compare the QFI amplification rate η versus scaled time $\omega_c t$ between the analytical results given in Eq. (41) and the numerical results of actual states with a fixed UDD pulse ($n = 20$). It can be seen from Fig. 5(a) that the analytical results are in good agreement with the numerical results in the pure state regimes ($\omega_c t < 5$). Figure 5(a) also indicates that large amplification rate η can be easily reached for large α by using UDD pulses. And the amplification rate η is $\simeq 50$ with respect to the initial state (CSS) when $\alpha = 0.05$ and $N = 100$. Another interesting behavior is that the large α (such as $\alpha = 0.05$) can maintain the QFI unchanged until the quantum state into the mixed states regime. In the mixed states regime the amplification rate is reduced, which implies that a larger number of UDD pulses is needed to extend the pure states preservation time, if one wants to maintain the maximal steady amplification rate.

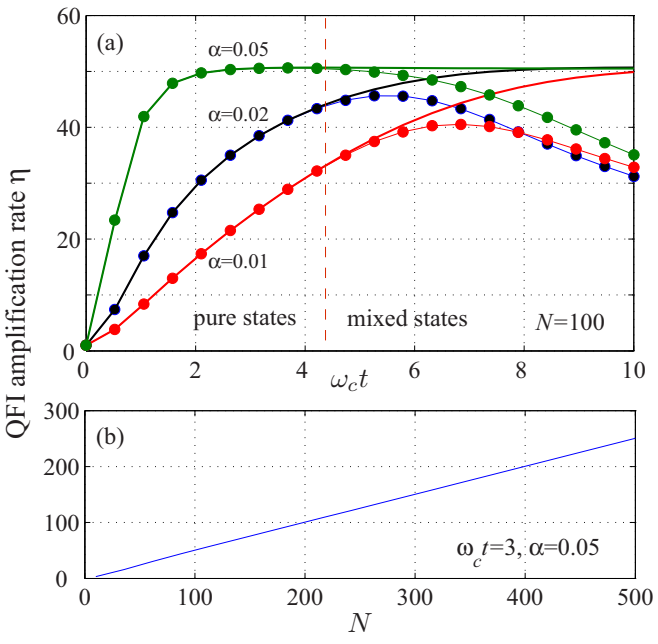

FIG. 5. (Color online) (a) QFI amplification rate η vs the scaled time $\omega_c t$ for different values of coupling strength α with the number of atoms $N = 100$. The solid lines are the analytical results of the pure state, while the solid circles lines present the numerical results of Eq. (40). In the pure states regime they fit well. (b) QFI amplification rate η as a function of atom number N at fixed time $\omega_c t = 4$ with $\alpha = 0.05$. Here the self-interaction is $\chi = 0.01$, the temperature is set as $T = 0.1\omega_c$, and the number of UDD pulses is $n = 20$.

The QFI amplification rate η as a function of atom number N at fixed scale time $\omega_c t = 4$ is given in Fig. 5(b). As shown, the amplification rate is proportional to the atom number N, and the scale factor is $\simeq 1/2$. It indicates that the amplification rate given in Eq. (41) has the maximum approximation value $\eta_{\max}(N) \simeq N/2$, thus the maximal QFI is $F_{\max} \simeq N^2/2$ in this case.

According to the quantum Cramér-Rao theorem, we know that the larger the QFI, the higher the precision of estimation is obtained. Thus, the dephasing-induced amplified QFI can greatly improve the parameter estimation precision; the best result is that it can enhance the phase sensitivity from SQL $\Delta\theta_{\min} = 1/\sqrt{N}$ to $\Delta\theta_{\min} = \sqrt{2}/N$, which is the same order of magnitude of the Heisenberg limit $(1/N)$. It should be pointed out that both SS and QFI are related to the precision in parameter estimation. The QFI determines the ultimate precision, but metrology based on SS is comparatively easy to implement in experiments [8].

V. CONCLUSION

In summary, we have studied the dephasing-assisted PPE enhancement in a two-component BEC system with DD pulses, through calculating dephasing-induced SS and QFI. We have found that the dephasing noise can improve PPE by inducing SS, and the DD pulses can maximize the improvement. We have compared the effects between PDD sequence and UDD sequence. Our results showed that the UDD sequence can work more efficiently, which can enhance the decoherence-induced SS to the limit of $\xi^2 \simeq N^{-2/3}$ more easily and it can amplify the QFI by a factor of $\simeq N/2$ for the initial state of CSS. It implied that the sensitivity $\Delta\theta$ of the estimated parameter θ can be enhanced from the SQL $1/\sqrt{N}$ to $\sqrt{2}/N$, which achieves nearly Heisenberg-limited precision $(1/N)$.

We would like to point out that we have subjected to the assumption of negligible effects of atom losses; although these will limit the achievable squeezing and affect the precision of metrology to some extent, our results highlight that there is no fundamental obstacle to improving the dephasing-assisted PEP. What is more, all the π control pulses are assumed to execute quickly and perfectly, during which the coupling with environment is negligible. In addition, we also have noted that the Heisenberg-limited precision estimation precision has been reached theoretically, via transforming the OAT into "two-axis twisting" [17,32] if some more complex control fields are employed. Finally, we expect that our idea might have promising applications in quantum metrology and be realized within current experiments.

ACKNOWLEDGMENTS

We are grateful to Professor Hongwei Xiong, Professor Hui Jing, and Professor Su Yi for useful discussions. X.W. acknowledges support from the NFRPC through Grant No.

2012CB921602 and the NSFC through Grants No. 11025527 and No. 10935010. L.M.K. acknowledges support from the 973 Program under Grant No. 2013CB921804, and the NSF under Grants No. 11375060 and No. 11075050. Q.S.T. acknowledges the China Postdoctoral Science Foundation (Grant No. 2013M541766).

APPENDIX A: DERIVATION OF THE DECOHERENCE FUNCTION $R(t)$

Here, we present a detailed derivation of the decoherence function $R(t)$. From Eq. (16), the reduced density matrix elements of the system can be obtained as

$$\rho^S_{m,l}(t) = \mathrm{Tr}_B[\langle m|U(t)\rho(0)U^{-1}(t)|l\rangle] = e^{-i\phi(t)(m-l)}e^{-i(m^2-l^2)\tilde{\Delta}(t)}\mathrm{Tr}_B\left\{\exp\left[(m-l)\sum_k(\alpha_k b_k^\dagger - \alpha_k^* b_k)\right]\rho_B(0)\right\}\rho_{m,l}(0) \quad \text{(A1)}$$

with $\alpha_k = -ig_k\int_0^t e^{i\omega_k s}\varepsilon(\tau)\,d\tau$ and $\phi(t) = \int_0^t \lambda\varepsilon(\tau)\,d\tau$.

To obtain the explicit expression of Eq. (A1), the main task becomes to calculate the expectation value of displacement operator

$$\Pi_k \mathrm{Tr}_B\left[D(z_k)\rho_B\right] = \mathrm{Tr}_B\left\{\exp\left[(m-l)\sum_k(\alpha_k b_k^\dagger - \alpha_k^* b_k)\right]\rho_B\right\} \quad \text{(A2)}$$

with $z_k = (m-l)\alpha_k$. Making use of the following formula [67]:

$$\mathrm{Tr}_B\left[D(z_k)\rho_B\right] = \exp[-(\langle n_k\rangle + 1/2)\,|z_k|^2], \quad \text{(A3)}$$

where $n_k = 1/(e^{\beta\omega_k}-1)$, we arrive at

$$\langle D(z_k)\rangle = \mathrm{Tr}_B\left[D(z_k)\rho_B\right] = \exp\left\{-(m-l)^2\int_0^\infty d\omega\, J(\omega)[2n(\omega)+1]F_n(\omega,t)\right\} = \exp[-(m-l)^2 R(t)]. \quad \text{(A4)}$$

In Eq. (A4), the function $F_n(\omega,t)$ is given as

$$\begin{aligned} F_n(\omega,t) &= |\varepsilon(\omega,t)|^2/2 = \frac{1}{2}\left|\int_0^t e^{i\omega\tau}\varepsilon(\tau)d\tau\right|^2 \\ &= \frac{1}{2}\left|\sum_{j=0}^{n}\int_0^t e^{i\omega\tau}(-1)^j\theta(\tau-t_j)\theta(t_{j+1}-\tau)d\tau\right|^2 = \frac{1}{2\omega^2}\left|1+(-1)^{n+1}e^{i\omega t}+2\sum_{j=1}^{n}(-1)^j e^{i\omega t_j}\right|^2. \end{aligned} \quad \text{(A5)}$$

Therefore, the decoherence function in Eq. (17) is obtained.

APPENDIX B: DERIVATION OF $f(\omega,t)$

In this appendix, we present the details of the derivation of Eq. (21). Based on Eqs. (11) and (13), we have

$$f(\omega,t) = \int_0^t d\tau\int_0^\tau d\tau'\varepsilon(\tau)\varepsilon(\tau')\sin[\omega(\tau'-\tau)] = [x^*(\omega,t)-x(\omega,t)]/(2i) = -\mathrm{Im}[x(\omega,t)], \quad \text{(B1)}$$

where $x(\omega,t)$ is given by

$$\begin{aligned} x(\omega,t) &= \int_0^t ds\,\varepsilon(\tau)e^{i\omega\tau}\int_0^\tau d\tau'\varepsilon(\tau')e^{-i\omega\tau'} = \sum_{m=0}^{n}\int_{t_m}^{t_{m+1}} ds(-1)^m e^{i\omega\tau}\int_0^\tau d\tau'\varepsilon(\tau')e^{-i\omega\tau'} \\ &= \sum_{m=0}^{n}\int_{t_m}^{t_{m+1}} d\tau\,(-1)^m e^{i\omega\tau}\left[\sum_{j=1}^{m}\int_{t_{j-1}}^{t_j} d\tau'(-1)^{j-1}e^{-i\omega\tau'} + (-1)^m\int_{t_m}^{\tau} d\tau' e^{-i\omega\tau'}\right] \\ &= -\frac{i}{\omega}\left\{\sum_{m=0}^{n}\int_{t_m}^{t_{m+1}} d\tau(-1)^m e^{i\omega\tau}\left[1+2\sum_{j=1}^{m}(-1)^j e^{-i\omega t_j}+(-1)^{m+1}e^{-i\omega\tau}\right]\right\} \\ &= \frac{1}{\omega^2}\left[1+(-1)^{n+1}e^{i\omega t}+2\sum_{m=1}^{n}(-1)^m e^{-i\omega t_m}\right] - \frac{2i}{\omega}\sum_{m=1}^{n}\sum_{j=1}^{m}\int_{t_m}^{t_{m+1}} ds(-1)^{m+j}e^{i\omega\tau}e^{-i\omega t_j} + it/\omega. \end{aligned} \quad \text{(B2)}$$

We therefore have

$$f_n(\omega,t) = \vartheta(\omega,t) + \mu(\omega,t) - t/\omega, \quad \text{(B3)}$$

with

$$\vartheta(\omega,t)=\frac{1}{\omega^2}\left[2\sum_{m=1}^{n}(-1)^m\sin(\omega t_m)+(-1)^{n+2}\sin(\omega t)\right],$$
$$\mu(\omega,t)=\frac{2}{\omega^2}\left\{\sum_{m=1}^{n}\sum_{j=1}^{m}(-1)^{m+j}(\sin[\omega(t_{m+1}-t_j)]-\sin[\omega(t_m-t_j)])\right\}, \tag{B4}$$

which is Eq. (21) of the main text.

APPENDIX C: QFI OF PURE STATES

Here, we will give the derivation of the QFI for the case of pure states. Based on Eq. (37) of the main text, we have

$$\mathbf{C}=4\begin{pmatrix}(\Delta J_x)^2 & \mathrm{cov}(J_x,J_y) & \mathrm{cov}(J_x,J_z)\\ \mathrm{cov}(J_x,J_y) & (\Delta J_y)^2 & \mathrm{cov}(J_y,J_z)\\ \mathrm{cov}(J_x,J_z) & \mathrm{cov}(J_y,J_z) & (\Delta J_z)^2\end{pmatrix}, \tag{C1}$$

with $\mathrm{cov}(J_m,J_l)=\frac{1}{2}\langle J_mJ_l+J_lJ_m\rangle-\langle J_m\rangle\langle J_l\rangle$.

When the UDD pulses are employed, we have $\phi(t)=\int_0^t\lambda\varepsilon(\tau)\,d\tau=0$ in Eq. (12). Following Eq. (16) and Ref. [15], the expectation values relevant in $\mathrm{cov}(J_m,J_l)$ can be obtained as

$$\begin{aligned}\langle J_xJ_y+J_yJ_x\rangle&=\mathrm{Im}\langle J_+^2\rangle=0,\\ \langle J_xJ_z+J_zJ_x\rangle&=\mathrm{Re}\langle J_+(2J_z+1)\rangle=0,\\ \langle J_yJ_z+J_zJ_y\rangle&=\mathrm{Im}\langle J_+(2J_z+1)\rangle,\end{aligned} \tag{C2}$$

with

$$\begin{aligned}\langle J_+(2J_z+1)\rangle&=iN(N-1)\cos^{N-2}[2\tilde{\Delta}(t)]\sin[\tilde{\Delta}(t)]/2,\\ \langle J_+\rangle&=N\cos^{N-1}[\tilde{\Delta}(t)]/2,\\ \langle J_+^2\rangle&=N(N-1)\cos^{N-2}[2\tilde{\Delta}(t)]/4,\end{aligned} \tag{C3}$$

and

$$\begin{aligned}&\langle J_x\rangle=N\cos^{N-1}[\tilde{\Delta}(t)]/2,\ \langle J_y\rangle=\langle J_z\rangle=0,\ \langle J_z^2\rangle=N/4,\\ &\langle J_x^2\rangle=(N(N+1)+N(N-1)\cos^{N-2}[2\tilde{\Delta}(t)])/8,\\ &\langle J_y^2\rangle=(N(N+1)-N(N-1)\cos^{N-2}[2\tilde{\Delta}(t)]|)/8.\end{aligned} \tag{C4}$$

Hence, the symmetric matrix $\mathbf{C}$ can be rewritten as

$$\mathbf{C}=4\begin{pmatrix}(\Delta J_x)^2 & 0 & 0\\ 0 & \langle J_y^2\rangle & \mathrm{cov}(J_y,J_z)\\ 0 & \mathrm{cov}(J_y,J_z) & \langle J_z^2\rangle\end{pmatrix}, \tag{C5}$$

and the maximal eigenvalue for Eq. (C5) can be obtained as

$$\lambda_{\max}=4\ \max\{(\Delta J_x)^2,\lambda_\pm\}, \tag{C6}$$

where

$$\begin{aligned}\lambda_\pm&=\frac{\langle J_y^2+J_z^2\rangle\pm\sqrt{\left(\langle J_y^2+J_z^2\rangle\right)^2+4\,\mathrm{cov}(J_y,J_z)^2}}{2},\\ (\Delta J_x)^2&=\frac{N}{4}\left(\frac{N+1}{2}+\frac{N-1}{2}\cos^{N-2}[2\tilde{\Delta}(t)]\right.\\ &\quad\left.-N\cos^{2N-2}[\tilde{\Delta}(t)]\right).\end{aligned} \tag{C7}$$

[1] T. L. Gustavson, P. Bouyer, and M. A. Kasevich, Phys. Rev. Lett. **78**, 2046 (1997).
[2] J. Fixler, G. Foster, J. McGuirk, and M. Kasevich, Science **315**, 74 (2007).
[3] A. D. Cronin, J. Schmiedmayer, and D. E. Pritchard, Rev. Mod. Phys. **81**, 1051 (2009).
[4] C. Gross, T. Zibold, E. Nicklas, J. Estève, and M. K. Oberthaler, Nature (London) **464**, 1165 (2010).
[5] M. F. Riedel, P. Böhi, Y. Li, T. W. Hansch, A. Sinatra, and P. Treutlein, Nature (London) **464**, 1170 (2010).
[6] N. Bar-Gill, D. D. Bhaktavatsala Rao, and G. Kurizki, Phys. Rev. Lett. **107**, 010404 (2011).
[7] J. Grond, U. Hohenester, I. Mazets, and J. Schmiedmayer, New J. Phys. **12**, 065036 (2010).
[8] J. Ma, X. Wang, C. P. Sun, and F. Nori, Phys. Rep. **509**, 89 (2011).
[9] J. Huang, S. Wu, H. Zhong, and C. Lee, *Annual Review of Cold Atoms and Molecules* (World Scientific, Singapore, 2013), Vol. 2, Chap. 7.
[10] P. Bouyer and M. A. Kasevich, Phys. Rev. A **56**, R1083 (1997).
[11] M. A. Kasevich, Science **298**, 1363 (2002).
[12] C. Orzel, A. K. Tuchman, M. L. Fenselau, M. Yasuda, and M. A. Kasevich, Science **291**, 2386 (2001).
[13] D. J. Wineland, J. J. Bollinger, W. M. Itano, and D. J. Heinzen, Phys. Rev. A **50**, 67 (1994).
[14] M. Kitagawa and M. Ueda, Phys. Rev. A **47**, 5138 (1993).
[15] G. R. Jin, Y. C. Liu, and W. M. Liu, New J. Phys. **11**, 073049 (2009).
[16] L. Pezze and A. Smerzi, Phys. Rev. Lett. **102**, 100401 (2009).
[17] Y. C. Liu, Z. F. Xu, G. R. Jin, and L. You, Phys. Rev. Lett. **107**, 013601 (2011).
[18] C. Simon and J. Kempe, Phys. Rev. A **65**, 052327 (2002).
[19] A. Andre and M. D. Lukin, Phys. Rev. A **65**, 053819 (2002).
[20] J. K. Stockton, J. M. Geremia, A. C. Doherty, and H. Mabuchi, Phys. Rev. A **67**, 022112 (2003).
[21] Y. Li, Y. Castin, and A. Sinatra, Phys. Rev. Lett. **100**, 210401 (2008).
[22] A. Sinatra, E. Witkowska, J.-C. Dornstetter, Y. Li, and Y. Castin, Phys. Rev. Lett. **107**, 060404 (2011).
[23] G. Watanabe and H. Makela, Phys. Rev. A **85**, 023604 (2012).
[24] X. Wang, A. Miranowicz, Y. X. Liu, C. P. Sun, and F. Nori, Phys. Rev. A **81**, 022106 (2010).

[25] L. Viola and S. Lloyd, Phys. Rev. A **58**, 2733 (1998).
[26] K. Khodjasteh and D. A. Lidar, Phys. Rev. A **75**, 062310 (2007).
[27] G. Gordon and G. Kurizki, Phys. Rev. Lett. **97**, 110503 (2006); G. Gordon, J. Phys. B: At. Mol. Opt. Phys. **42**, 223001 (2009).
[28] G. S. Uhrig, Phys. Rev. Lett. **98**, 100504 (2007); New J. Phys. **10**, 083024 (2008).
[29] W. Yang and R. B. Liu, Phys. Rev. Lett. **101**, 180403 (2008).
[30] J. F. Du, X. Rong, N. Zhao, Y. Wang, J. H. Yang, and R. B. Liu, Nature (London) **461**, 1265 (2009).
[31] X. Rong, P. Huang, X. Kong, X. Xu, F. Shi, Y. Wang, and J. Du, Europhys. Lett. **95**, 60005 (2011).
[32] A. Z. Chaudhry and J. Gong, Phys. Rev. A **87**, 012129 (2013); **86**, 012311 (2012).
[33] Y. Pan, H. T. Song, and Z. R. Xi, J. Phys. B: At. Mol. Opt. Phys. **45**, 205504 (2012).
[34] Q. S. Tan, Y. Huang, X. Yin, L. M. Kuang, and X. Wang, Phys. Rev. A **87**, 032102 (2013).
[35] J. M. Taylor, P. Cappellaro, L. Childress, L. Jiang, D. Budker, P. R. Hemmer, A. Yacoby, R. Walsworth, and M. D. Lukin, Nat. Phys. **4**, 810 (2008).
[36] G. de Lange, D. Ristè, V. V. Dobrovitski, and R. Hanson, Phys. Rev. Lett. **106**, 080802 (2011).
[37] G. Goldstein, P. Cappellaro, J. R. Maze, J. S. Hodges, L. Jiang, A. S. Sørensen, and M. D. Lukin, Phys. Rev. Lett. **106**, 140502 (2011).
[38] L. T. Hall, C. D. Hill, J. H. Cole, and L. C. L. Hollenberg, Phys. Rev. B **82**, 045208 (2010).
[39] C. W. Helstrom, *Quantum Detection and Estimation Theory* (Academic, New York, 1976).
[40] S. L. Braunstein and C. M. Caves, Phys. Rev. Lett. **72**, 3439 (1994).
[41] V. Giovannetti, S. Lloyd, and L. Maccone, Nat. Photon. **5**, 222 (2011).
[42] Z. Sun, J. Ma, X. M. Lu, and X. Wang, Phys. Rev. A **82**, 022306 (2010).
[43] J. Ma, Y.-x. Huang, X. Wang, and C. P. Sun, Phys. Rev. A **84**, 022302 (2011).
[44] G. Ferrini, D. Spehner, A. Minguzzi, and F. W. J. Hekking, Phys. Rev. A **84**, 043628 (2011).
[45] Y. Huang, W. Zhong, Z. Sun, and X. Wang, Phys. Rev. A **86**, 012320 (2012).
[46] V. Giovannetti, S. Lloyd, and L. Maccone, Science **306**, 1330 (2004); Phys. Rev. Lett. **96**, 010401 (2006).
[47] S. F. Huelga, C. Macchiavello, T. Pellizzari, A. K. Ekert, M. B. Plenio, and J. I. Cirac, Phys. Rev. Lett. **79**, 3865 (1997); A. W. Chin, S. F. Huelga, and M. B. Plenio, *ibid.* **109**, 233601 (2012).
[48] D. S. Hall, M. R. Matthews, J. R. Ensher, C. E. Wieman, and E. A. Cornell, Phys. Rev. Lett. **81**, 1539 (1998).
[49] M. R. Matthews, D. S. Hall, D. S. Jin, J. R. Ensher, C. E. Wieman, E. A. Cornell, F. Dalfovo, C. Minniti, and S. Stringari, Phys. Rev. Lett. **81**, 243 (1998).
[50] A. Micheli, D. Jaksch, J. I. Cirac, and P. Zoller, Phys. Rev. A **67**, 013607 (2003).
[51] P. O. Fedichev, M. W. Reynolds, and G. V. Shlyapnikov, Phys. Rev. Lett. **77**, 2921 (1996).
[52] B. D. Esry, C. H. Greene, and J. P. Burke, Phys. Rev. Lett. **83**, 1751 (1999).
[53] M. W. Jack, Phys. Rev. Lett. **89**, 140402 (2002).
[54] B. Borca, J. W. Dunn, V. Kokoouline, and C. H. Greene, Phys. Rev. Lett. **91**, 070404 (2003).
[55] C. P. Search, W. Zhang, and P. Meystre, Phys. Rev. Lett. **92**, 140401 (2004).
[56] K. Pawłowski and K. Rzażewski, Phys. Rev. A **81**, 013620 (2010).
[57] P. J. Y. Louis, P. M. R. Brydon, and C. M. Savage, Phys. Rev. A **64**, 053613 (2001).
[58] L. M. Kuang, Z. Y. Tong, Z. W. Ouyang, and H. S. Zeng, Phys. Rev. A **61**, 013608 (1999).
[59] D. A. R. Dalvit, J. Dziarmaga, and W. H. Zurek, Phys. Rev. A **62**, 013607 (2000); J. Ruostekoski and D. F. Walls, *ibid.* **58**, R50 (1998); J. Anglin, Phys. Rev. Lett. **79**, 6 (1997).
[60] W. Wang, L. B. Fu, and X. X. Yi, Phys. Rev. A **75**, 045601 (2007).
[61] S. Giorgini, L. P. Pitaevskii, and S. Stringari, Phys. Rev. Lett. **80**, 5040 (1998).
[62] H. D. Politzer, Phys. Rev. A **54**, 5048 (1996).
[63] H. Xiong, S. Liu, G. Huang, and Z. Xu, Phys. Rev. A **65**, 033609 (2002); H. Xiong, S. Liu, and G. Huang, *ibid.* **67**, 055601 (2003).
[64] P. Navez, D. Bitouk, M. Gajda, Z. Idziaszek, and K. Rzażewski, Phys. Rev. Lett. **79**, 1789 (1997).
[65] T. Vorrath, T. Brandes, and B. Kramer, Chem. Phys. **296**, 295 (2004).
[66] T. Vorrath and T. Brandes, Phys. Rev. Lett. **95**, 070402 (2005).
[67] H. P. Breuer and F. Petruccione, *The Theory of Open Quantum Systems* (Oxford University Press, Oxford, 2002).
[68] S. Blanes, F. Casas, J. A. Oteo, and J. Ros, Phys. Rep. **470**, 151 (2009).
[69] A. O. Caldeira and A. J. Leggett, Ann. Phys. (NY) **149**, 374 (1983).
[70] J. B. Yuan, L. M. Kuang, and J. Q. Liao, J. Phys. B: At. Mol. Opt. Phys. **43**, 165503 (2010).
[71] T. Tanaka, G. Kimura, and H. Nakazato, Phys. Rev. A **87**, 012303 (2013).